Indian Society for
Non-Destructive Testing
Hyderabad Chapter

Proc. National Seminar on
Non-Destructive Evaluation
Dec. 7 - 9, 2006, Hyderabad

Thermographic Inspection of Composite Materials

K. Srinivas, A.O. Siddiqui and J. Lahiri
Directorate of Advanced Composites, Advanced Systems Laboratory, DRDO,
Hyderabad-500 058
e-mail: vasu72@rediffmail.com

Abstract

Thermography is a non-contact NDT technique for inspection of materials in wide application areas, including corrosion detection in metals, and delamination, porosity and moisture detection in composite materials. Composites often are highly anisotropic in nature. This anisotropy coupled with low thermal diffusivity in thickness direction, severely restricts detection of deeper defects in composite materials.

In the present work, a systematic methodology has been presented for detection of defects in composite materials. The material under consideration is carbon-epoxy, which has high thermal anisotropy because of carbon fibers. Carbon-epoxy laminates with Teflon inserts of varying depth were fabricated for experimental studies. Both one sided and two sided test methods were explored.

Based on numerical solution of the heat conduction problem, the optimum combination of heat flux, heating time and observation time for 'best defect detectibility' was worked out in each case, assuming zero noise condition. Using these parameter windows as the guidelines, experiments were conducted and the results were compared with the corresponding theoretical predictions. Noise characteristics for each laminate-test configuration were studied experimentally. The same was used for determining the expected limits of defect detection in presence of normal experimental noise. Finally, standard data processing algorithms e.g polynomial fitting and phase imaging were used for enhancing contrast and visualizing the defects.

Keywords: *Thermography, Infrared, CFRP, Delamination, Phase imaging*

1. Introduction

Thermography is now a popular non-destructive testing method for detecting defects in composite structures. Active thermography method for composites is well reported in literature [1-6]. An active thermography system consists of a heater unit for controlled heating of the component under test, an Infra-red (IR) camera for capturing the surface temperature evolution of the component, and a data acquisition system for acquiring the corresponding IR images over a specific period of time. However, this method has not been applied much to thick composite structures (thickness of the order of 15 mm) as heat propagation through large thickness results in poor defect definition. Our earlier papers have described optimization of parameters like heat flux, heating time and observation time [7-8]. However, actual experimental conditions differ from the theoretical

predictions, which deal essentially with the idealized noise-free signals. Non-uniform emissivity, uneven heating of the test surface and variation in thermal properties of the test material are some of the crucial factors in experimental thermography.

Optimum conditions for thick composites have to be determined theoretically, to avoid doing large number of experiments to arrive at the best combination of heat flux and heating time. This is not reported much in literature though several researchers have reported thermography inspection of carbon fiber reinforced plastics (CFRP). Limitations of thermography inspection of composites are enhanced due to thermal anisotropy of CFRP, arising because of higher conductivity of carbon fibers and the layered structure of the composite.

In this paper, we report optimization of thermography NDT parameters for thick (CFRP) composite laminate having thickness of 15mm. Optimization with respect to heat input and heating time for defect detection is done theoretically, before conducting the experiments. This brings out the restrictions in selecting parameter windows and essentially sets the theoretical upper limit of detectable defect's depth under ideal noise-free condition. Subsequently, following issues have been investigated and discussed with respect to defect detectability:

(a) Effect of noise on defect detection

(b) Noise characterization

(c) Defect detection enhancement using data processing methods

(d) Determination of defect detection limit for 15 mm thick laminate in one-sided inspection, based on experimental data and analysis.

2. Experimental

Active thermography inspection of composites is done by two methods, namely one-sided inspection and two-sided inspection. In one-sided method, composite laminate is heated using an external heating source and transient IR images are captured from the same side while heater is switched off (IR images are captured immediately after the heater is switched off, with minimum loss of time). In this method, the advantage of capturing images from the same side of heating lies in easy accessibility and in subsequent defect characterization. In two-sided inspection, the camera and the heater are placed on two sides of the laminate, facing each other. The laminate is heated from one side and IR images are captured from the other side. The present work covers both these methods; though it focuses primarily on single sided test.

A Carbon–epoxy (0-90 cross ply) laminate (15 mm thickness; size: 300 x 300 mm) with embedded Teflon defects (lateral and longitudinal positions along with their depths are shown in Fig.1) was chosen for the study. Teflon defects of 20 mm diameter and 0.1 mm thickness were embedded during fabrication. Prior to thermography inspection, the embedded defects were detected using ultrasonic pulse echo method and their depths were determined. All the defects were detectable by the ultrasonic method and their positions were clearly identified.

Thermography inspection of the test laminate was done using a 24 kW step heater as heat source. The step heater can be used with different test configurations by varying the heat input (percentage power can be varied from 1% to 100% in steps of 1%) and heating time (time in seconds can be varied from 1 sec to 20 seconds in steps of 1 sec). Infrared camera (wavelength 8-9 μm and resolution of 0.03 K) has been used for capturing the IR

images. It is possible to vary heat input and heating time in steps to obtain 'best defect detectability', which depends on the material being tested, its thickness and depth of the defect (size and thickness of defect are kept constant). Details of the laminate under study are given below:

Material Under study: Carbon Epoxy Laminate (0-90^0 cross ply)

Defect Material: Teflon

Laminate Thickness: 15mm

Laminate Dimensions: 300 X 300mm

Defect Thickness: 0.1mm

Defect Dimensions: 20mm diameter circular

Thermal Diffusivity (m^2/sec):

Carbon-Epoxy 2.62 x 10^{-6} (x and y direction)

4.60 x 10^{-7} (z direction)

Teflon 1.39 x 10^{-7} (isotropic)

3. Theoretical Modeling

Theoretical modeling has been done by taking laminate thickness, defect depths, defect size, defect thickness and material properties as inputs for the modeling program. For theoretical modeling, Thermocal 6L program (make: Institute of Introscopy, Tomsk Polytechnic, Russia) has been used. All the above inputs were given to the program to generate the time-temperature profiles corresponding to each defect at a particular depth. Theoretical estimates for temperature difference between defect and non defect regions (called signal) were made, using different sets of heat input values and heating times to determine the optimum conditions for experiments. The other important parameter studied is running contrast (defined as signal divided by non-defect zone's temperature). For the best defect detectability, signal and contrast both must be high enough to detect the defect. However, for achieving maximum signal, arbitrary increase in input heat flux is not allowed, since the maximum temperature on the laminate should be less than the destructive temperature of the composite. It may be mentioned here that theoretically (i.e under zero noise condition) running contrast is independent of heat flux. Details of theoretical analysis for determination of optimized experimental parameters are explained in subsequent sections.

3.1 Optimization Methodology

A sub-surface defect can be subjected to thermographic inspection, if the temperature signal caused by such a defect meets the following three necessary conditions:

3.1.1 Condition 1

At any point on the sample, in particular on its front surface, the temperature must not exceed the degradation temperature T_{dest} of the material, i.e. $T_{max} < T_{dest}$ (T_{dest} is 120^0C). Since sample temperature is linearly proportional to the absorbed energy W, this condition limits either heating power Q or heating duration t_h (note that W=Q. t_h).

3.1.2 Condition 2

A defect should generally produce a signal-to-noise ratio higher than unity (SNR>=1). The noise consists of additive (IR detector noise and irradiation from ambient) and multiplicative noise (structural noise). However, in idealized noise-free condition considered here for initial theoretical analysis differential temperature signal ΔT must be higher than the temperature resolution (ΔT_{res}) of IR

thermographic system, i.e. $\Delta T >= \Delta T_{res}$ should be satisfied for defect detection.

3.1.3 Condition 3

IR thermographic systems can be characterized by their time resolution, i.e. by the image acquisition rate f, which must be high enough to ensure a reasonable number of images before an optimum observation time t_m is reached.

In our case, IR camera used for thermography inspection has temperature resolution of 0.03^0C. Frame capture rate used is 50 Hz, which is high enough to meet condition 3 easily, without any concern. For theoretical modeling of the above-mentioned laminate, defects at each depth are simulated (varying heat flux and heating time) and temperature, signal and contrast data are calculated. This information is utilized in parameter optimization with above-mentioned constraints. Table 1 and Table 2 show theoretical estimation of signal at different heat input values and heating times for a defect of 20 mm diameter at depth of 1.5 mm and 6 mm respectively.

In Table 1 and Table 2, all the signal values shown in bold with underline are having conditions (heat flux and heating time), which result in surface temperatures exceeding the maximum permissible temperature of 120^0C for the test laminate. Hence, these conditions cannot be used for experiments as per condition 1. In the same tables, combinations of heat flux and heating time resulting in signal value less than the camera resolution (0.03^0C) are written in bold italics. Therefore, these combinations are also not acceptable as per condition 2. Now, the remaining combinations resulting in maximum signal values exceeding resolution of camera (0.03^0C) and surface temperature less than 120^0C may be considered further for defect detection.

Out of the above sets of parameters (which are acceptable as per 'T & ΔT criteria'), that particular heat flux/ heating time combination which produces maximum running contrast (C^{run}) should logically be the best choice for defect detection. However, it needs to be emphasized that this criterion, based on the computed values of running contrast will hold good, only under idealized zero-noise condition. Under all practical experimental conditions, presence of noise is expected to introduce additional complexities.

Theoretically, (i.e. by definition; under noise free condition) running contrast is independent of heat flux, but depends on heating time. Lower the heating time higher is the running contrast. However, low heating time results in low signal; hence, along with low heating time, heat flux should be kept reasonably high. Now back to Table 2 (for 6 mm depth embedded teflon defect) it is observed that the acceptable parameter windows at 18000 W/m^2 and 20000W/m^2 with 10 seconds of heating time in each case, are too narrow and precarious for practical application. Because slight overheating may push the laminate temperature towards degradation, while slight under heating is expected to produce weak signal, lower in magnitude than the camera resolution. In this context, a reasonable parameter window extending from 15000 W/m^2 (10 sec) to 15000 W/m^2 (20 sec) was tentatively selected and further explored, on the basis of its median value of 15000 W/m^2 (15 sec) as explained below.

It is well known that the experimental value of running contrast for a particular defect (i.e C^{run} measured experimentally in presence of noise) actually varies under changing heat flux, attaining its maximum at a particular heat flux value and decreasing thereafter [8]. A typical experimental running contrast versus heat flux plot for the defect at 1.5 mm depth,

generated through a series of experiments is presented in Fig 2.

According to this data, the optimum heating condition for detection of 1.5 mm deep defect is expected to be 15 kW/m^2 (15 sec). However, during the same experiment it was also observed that the surface temperature above this defect, though still below the theoretical upper limit of 120^{0}C, was tending to be high (>90^{0}C). This was a cause of practical concern. In subsequent set of experiments, heat flux was therefore arbitrarily reduced to 12 kW/m^2, while heating time was still maintained at 15 sec. The same heat input was used for investigating all other Teflon inserts embedded in the same laminate. Details of these experiments along with a discussion on the effects of noise, are present in the following sections.

Computation of T and ΔT values carried out for similar teflon inserts located at depths larger than 7.9mm in 15 mm thick CFRP laminate has further revealed that whatever may be the combination of heat flux and heating time values, it is impossible to avoid either getting ΔT less that camera resolution or getting the surface temperature greater than destructive temperature of the laminate. The computational approach thus has brought out clearly the maximum limit of defect detection under noise free condition as 7.9 mm (depth). This limit is expected to get restricted further in presence of noise (i.e under all practical situations). The same has been investigated in this paper by experimental thermography.

3.2 Noise Characterization

Thermal noises, namely additive noise and multiplicative noise are found to be major concerns in thermography. Additive noise is composed of spurious unwanted signals contributed by the reflections from the heater, the camera noise and the noise due to surrounding heat sources. Multiplicative noise is the noise (spurious unwanted signals) contributed by the variation in surface emissivity. Multiplicative noise may be eliminated to some extent by coating the test material with uniform emissivity black paint. Noise of a thermography experiment is defined by noise contrast (C_n), which is calculated as follows:

$$C_n = \sigma_n / T_{nd} \qquad (1)$$

σ_n is noise standard deviation (standard deviation of temperature within non-defect region or σ_{nd}) and T_{nd} is the average temperature of non-defect region. In general, C^{run}/C_n ratio is time-dependent, and the time when its maximum appears is often regarded as the optimum observation time. In some cases, C_n is approximately independent of time and thus characterizes a test material in a particular experiment [9]. In the present case, running contrast obtained from experimental studies (under normal noise condition) was plotted as function of heat flux (Fig. 2). The heat flux value, at which the contrast attains maxima, is taken as the best heat flux for the particular defect. It was further reported in [8] that, under this best heat flux condition, the running contrast shows relatively weak dependence on heating time.

Signal to noise ratio (SNR) is known as an important parameter, which determines defect detectability under a set of experimental conditions. In this case, the following formula has been adopted for calculating SNR

$$SNR=T_d-T_{nd}/\sigma_{nd} \qquad (2)$$

Where, T_d is the average temperature of the defect i.e average of all temperature values measured within specified defect area and σ_{nd} is standard deviation of temperature within specified non-defect area [9]. It may also be noted that SNR is

equal to the ratio of C^{run} and C^{noise} (equation 1)

4 Results and Discussion

4.1 Comparison of Theoretical and Experimental Results

The test laminate (Fig. 1) with embedded teflon inserts was experimentally inspected by one sided transient thermography method using the optimized heat flux and heating time. Fig. 3 shows the raw IR image of the laminate at a particular time frame. It is observed that shallow defects at 1.5 mm depth are clearly visible, whereas defects at 2.25 and 3mm depth are faintly visible in the raw thermogram. Defects at 3.75mm, 4.5mm and 5.25mm depth are lost in the noise due to weak signal. As per the theoretical predictions, defects of size 20 mm diameter present upto a depth of 7.9 mm should appear. However, in the experimental results the defects beyond 3 mm are faintly visible. The signal due to deeper defects being weaker than the noise, these defects appear to be lost in the background noise in raw thermography images.

In order to improve defect detectability, data processing methods had to be adopted. There are several data processing methods such as polynomial curve fitting, logarithmic curve fitting, normalization and phase imaging. Advantages of using data processing methods are, (i) increased signal to noise ratio (ii) decreased computation time (iii) improved defect detectability. Standard methods of data processing such as data compression, polynomial fitting, logarithmic fitting, normalization and phase imaging are well reported in literature [10-12].

Phase imaging method has been used in this case to improve defect detectability**.** Phase imaging is typically used as first method for defect detection, as deeper defects tend to appear in low frequency FFT images. Phase image of the test data is shown in the Fig. 4. It is observed that the defects upto a depth of 3.75 mm are clearly visible. Defects at 4.5 and 5.25 are faintly visible. This may be attributed to the signal to noise ratio (SNR) being lower for these defects (SNR is discussed in detail in subsequent sections).

Another method to eliminate additive noise is by smoothing the data**,** which eliminates unwanted up and downs in the raw data. Method used in the present study is the logarithmic fitting of pixel values as a function of time. In this method, data of each pixel is fitted to a logarithmic polynomial, and then the fitted coefficients of this polynomial are used to recover back the thermography data. Another advantage of curve fitting is that, it makes it possible to find the derivatives of the experimental data. Otherwise, if the derivative is found on raw data itself, any non-uniform pixel or noise component may make the derivative unstable [10].

First derivative of the fitted data was also determined, and one of the best visible frames is given in Fig. 5**.** 1st derivative of the data enhances the features which appear in transient condition, such as defects which are shallow and appear for short interval, and anomalies which have sharp changes with time. From Fig. 5 we see that the defects upto a depth of 5.25 mm are clearly visible.

It should be noted, that in the Fig.5, two defects at the same depth 1.5mm, appear with widely different intensities. As these are at the same depth and have same dimensions, they are expected to appear with same intensity and at the same time. One possibility of this behavior may be the presence of air above or below the defect. This was probed further by comparing the experimental signal values with theoretically predicted signal values.

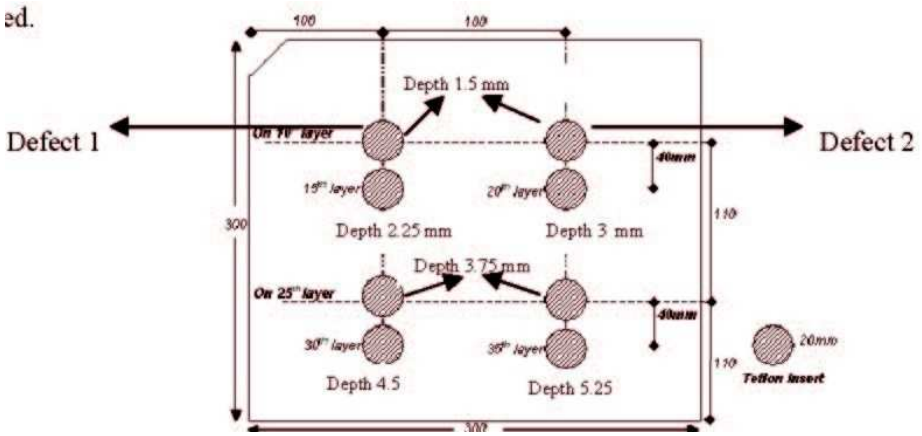

Fig. 1: Carbon-epoxy test laminate (total 100 layers) with embedded Teflon inserts at different depths

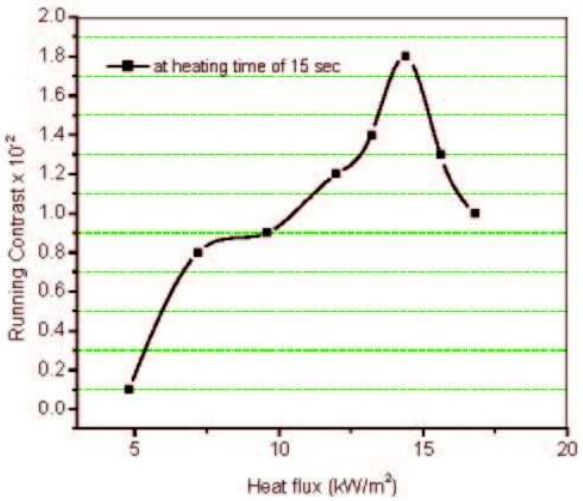

Fig. 2: Running contrast of defect at 1.5 mm depth as a function of heat flux

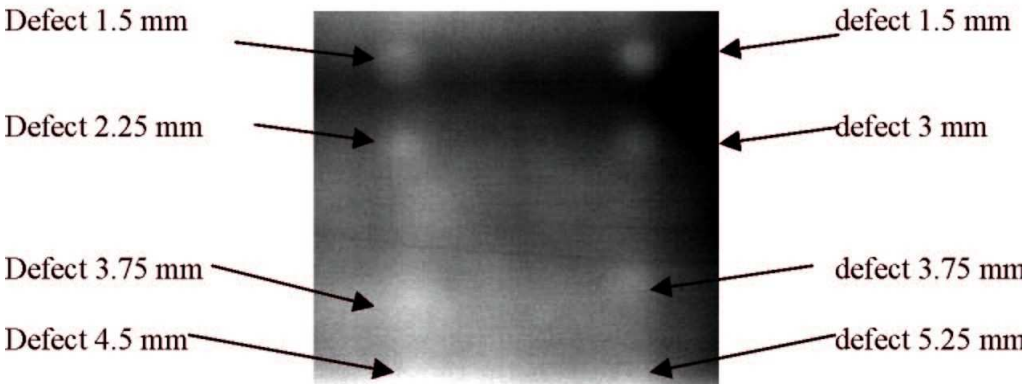

Fig. 3: IR thermography raw image of one-sided inspection of laminate (configuration shown in Fig. 1) with embedded teflon inserts at different depths

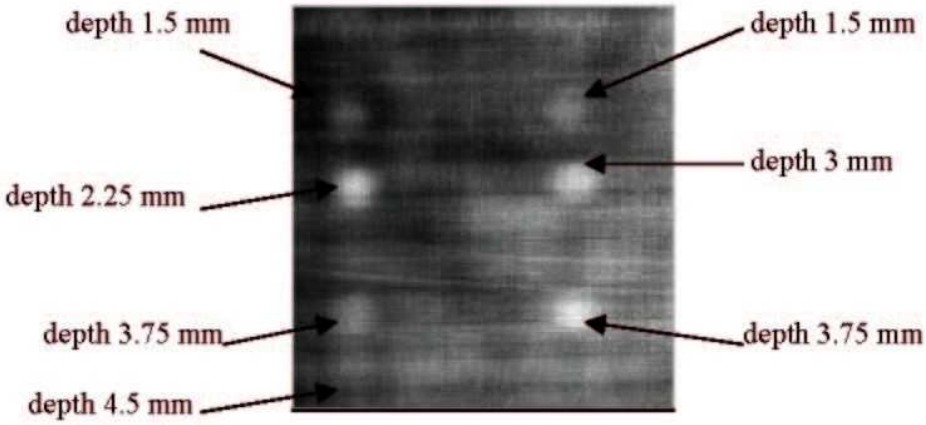

Fig. 4: Phase image of test laminate showing improved detectability of defects at different depths

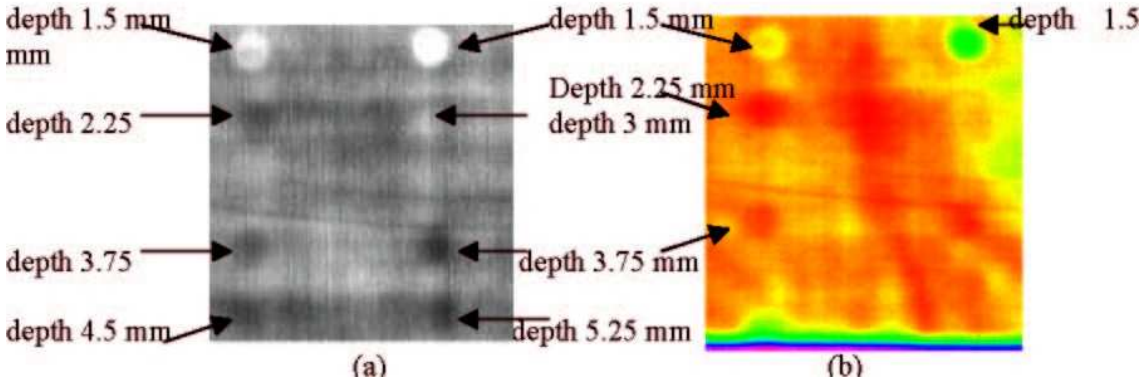

Fig. 5: I[st] derivative of the logarithmic fitted data of the test laminate in one sided inspection (a) gray scale processed image (b) color processed image

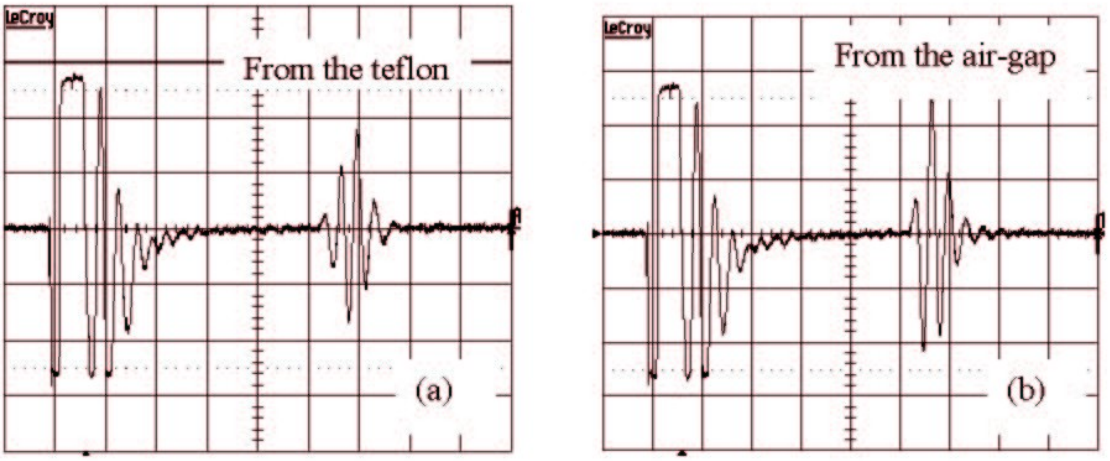

Fig. 6: (a) Ultrasonic PET data of teflon defect (defect 1) without air-gap (using krautkramer USIP 12 flaw detector and 5 MHz probes) (b) Ultrasonic PET data of teflon defect (defect 2) with air-gap (using same setup)

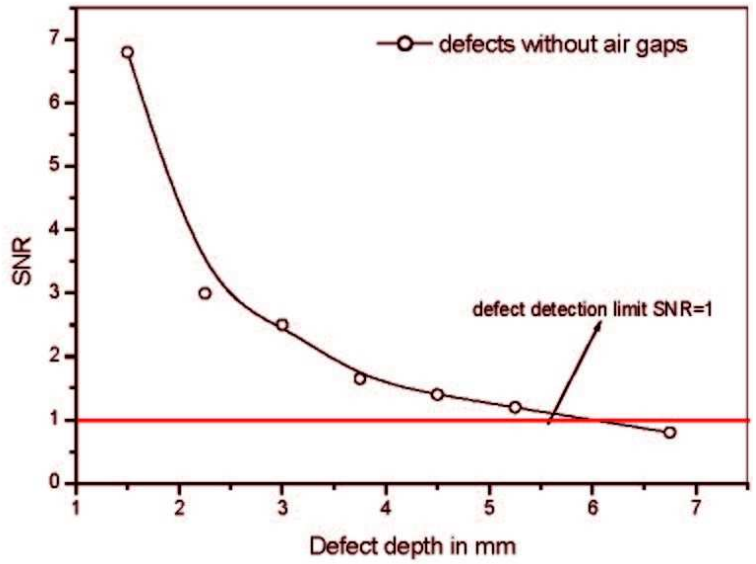

Fig. 7: SNR as a function of defect depth for CFRP laminate with teflon inserts (20 mm dia and 0.1 mm thickness) during one sided inspection. *Note: defect located at 6.75 mm depth in a different laminate has also been included in the figure for meaningful comparison

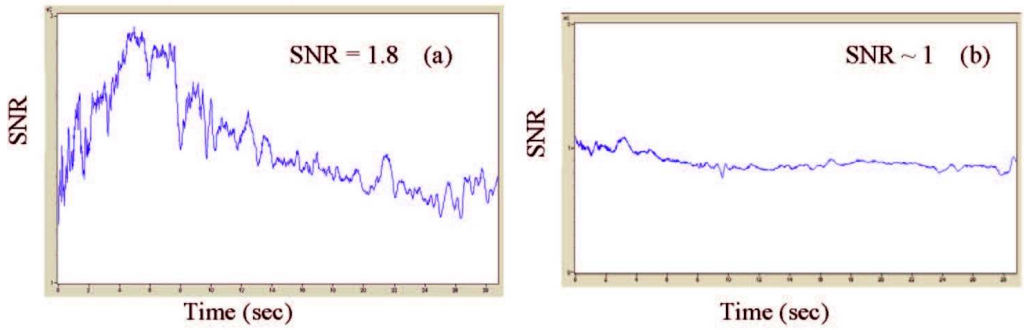

Fig. 8: (a) and 8(b) show SNR of shallow defect (2.25 mm depth) and deeper defect (5.25 mm depth)

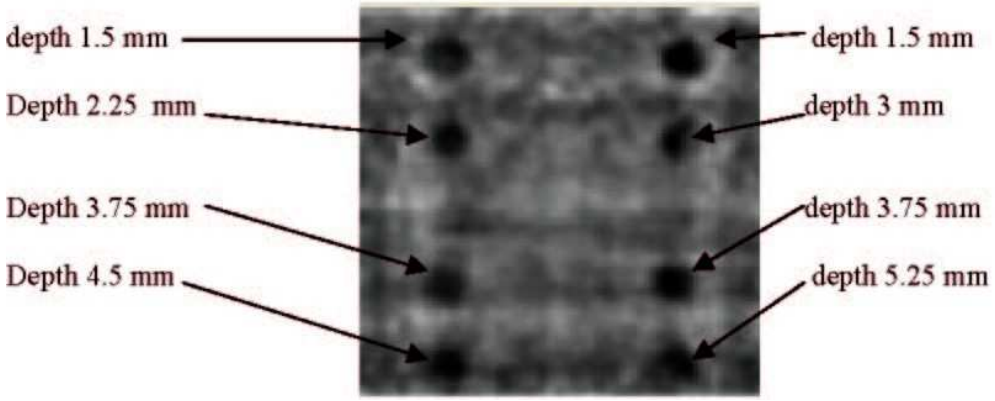

Fig. 9: IR thermography raw image of the test laminate in two-sided inspection

Table 1: Determination of Optimized parameters for defect detection for defect of 20 mm dia at 1.5 mm depth (Table below gives maximum signal values corresponding to different heat flux and heating time)

	2000	**5000**	**8000**	**10000**	**12000**	**15000**	**18000**	**20000**	**22000**	**24000**
2 sec	0.036	0.084	0.134	0.168	0.201	0.252	0.302	0.336	0.369	0.403
5	0.076	0.190	0.304	0.381	0.457	0.571	0.115	0.762	0.838	0.914
10	0.123	0.309	0.195	0.619	0.742	0.928	1.114	1.238	**1.361**	**1.485**
15	0.149	0.373	0.597	0.747	0.896	1.120	**1.344**	**1.494**	**1.643**	**1.792**
20	0.170	0.425	0.680	0.851	1.021	1.28	**1.531**	**1.702**	**1.872**	**2.042**
25	0.182	0.457	0.731	0.914	1.096	**1.371**	**1.645**	**1.828**	**2.010**	**2.193**
30	0.192	0.480	0.768	0.960	**1.152**	**1.440**	**1.728**	**1.920**	**2.112**	**1.304**

Table 2: Determination of Optimized parameters for defect detection for defect 20 mm dia at 6mm depth (Table below gives maximum signal values corresponding to different heat flux and heating time)

Heat flux W/m^2 Heating time	**2000**	**5000**	**8000**	**10000**	**12000**	**15000**	**18000**	**20000**	**22000**	**24000**
2 sec	***0.0009***	***0.002***	***0.003***	***0.004***	***0.005***	***0.006***	***0.008***	***0.009***	***0.009***	***0.010***
5 sec	***0.002***	***0.005***	***0.009***	***0.011***	***0.013***	***0.016***	***0.020***	***0.022***	***0.024***	***0.027***
10 sec	***0.004***	***0.011***	***0.018***	***0.022***	***0.027***	0.033	0.040	0.045	**0.049**	**0.054**
15 sec	***0.006***	***0.016***	***0.026***	0.033	0.040	0.050	**0.060**	**0.067**	**0.073**	**0.080**
20 sec	***0.008***	***0.022***	0.035	0.044	0.052	0.071	**0.079**	**0.088**	**0.097**	**0.106**
25 sec	***0.011***	***0.029***	0.047	0.059	**0.066**	**0.089**	**0.107**	**0.119**	**0.131**	**0.143**
30	***0.012***	0.032	0.051	0.064	**0.077**	**0.096**	**0.115**	**0.128**	**0.141**	**0.154**

Table 3: Comparison of signal and contrast values of Teflon defects at 1.5 mm depth (20 mm dia) using 12000 W/m^2 for 15 sec.

	Defect 1(without air gap)		Defect 2 (with air-gap)	
	Theoretical Experimental	Theoretical*		Experimental
Maximum signal	0.896	0.723	0.896	1.984
Maximum contrast	0.025	0.011	0.025	0.038
Time of maximum signal	17.1	16.7	17.1 Peak	missed (early appearance)
Time of maximum contrast	18.1	17.6	18.1 Peak	missed (early appearance)

* assuming no air gap is present

Table 3 shows comparison of experimentally found maximum signal and contrast value and their time of appearance with those of theoretically predicted values. The signal over the defect at a depth of 1.5 mm should have a maximum signal value of 0.896 in one sided inspection method (heat flux 12 kW/m2 for 15 sec). Experimental values showed that for defect 1 (see Fig.1), maximum signal value and time of appearance are of the same order as predicted; whereas, for defect 2, experimental values of signal is much more than the predicted value. This mismatch in maximum signal and early appearance of defect 2 was further studied with complementary ultrasonic NDT method. Fig.6 (a) shows ultrasonic pulse echo signal over defect 1. The Signal shows reflection due to Teflon. Fig.6 (b) shows ultrasonic pulse echo signal over the defect 2. The signal in this case shows leftward shift of the defect peak and its phase reversal, indicating the presence of air above Teflon. Thus, defect 1 according to ultrasonic data was free of air gap and the signal maximum was matching reasonably well with theoretical estimation, whereas, for defect 2, presence of air-gap over the Teflon insert has resulted in higher intensity signal (heat entrapped above thermally insulating air gap).

It is observed that the time of appearance of maximum signal and contrast are matching well with the theoretical predictions for defect 1. For defect 2, time of appearance of maxima was missed in early frames, because the presence of air over Teflon makes the defect shallow. In this laminate, all other defects (depths of 2.25, 3, 3.75, 4.5 and 5.25 mm) were found to be free of air gaps.

4.2 Signal to Noise Ratio and Defect Detection Limits:

Estimation of signal to noise ratio of each defect as a function of the defect depth is another way to estimate defect detectability limits. In this case, SNR for each defect was calculated using equation 2 mentioned earlier for one-sided inspection of the test laminate at heat flux of 12000 kW/m^2 for 15 sec. Under these conditions, difference of average temperature of defect area and non-defect area was divided by the standard deviation of the non-defect area to estimate SNR for a particular defect. Defects with air-gap were found to show higher SNR. As for example, defect at 1.5 mm depth with air-gap (defect 2, see fig 1 and fig 6(b)) has SNR value of 17, whereas defect at same depth without air-gap (defect 1, see fig 1 and fig 6(a)) has SNR value of 6.8. Higher SNR for defect with air-gap than defect without air-gap is attributed to higher signal (see table 3 for comparison). Corresponding defect appearance times in transient condition also vary. Hence in the determination of defect detection limits for the test laminate, only SNR of defects without air-gaps were considered.

Figure 7 shows the SNR as a function of defect depth for the experimental test laminate. It is estimated that under the present experimental conditions, the defects at a depth of 5.25 mm and above have SNR values less than 1 (C^{noise} ~1%). Hence, defects having SNR <1 are not detectable (see fig.4) i.e SNR value of greater than unity will specify the detection limit. In Fig. 7, the red line indicates the defect detectability limit for thermography of 15 mm thick laminate in one-sided inspection under the above-defined conditions with Teflon inserts.

SNR also varies as a function of time and attains a peak value (which may coincide with time of maximum signal). Figure 8 (a) & (b) show the SNR as a function of time for shallow defect (1.5 mm depth without air gap) and deeper defect (5.25 mm depth). For shallow defect without air-gap SNR has a peak value of ~1.8, whereas, for deeper defect SNR is just above 1. Hence, it is faintly detectable.

5. Two Sided Inspection

Another method of detecting defects as described earlier is two-sided inspection. Fig. 9 shows IR thermography (raw image) of test laminate by two-sided test, using heat flux of 24000w/m^2 for 5 sec. Since detectability of defects by this method was found to be extremely good, deeper defects were also explored by keeping the same CFRP laminate upside down vis-à-vis the heating system. Typical raw image of defects detected in normal configuration is presented in Fig 9. All defects are detectable by this method. The deepest defect detectable was at a depth of 13.5 mm in upside down configuration of the same laminate. Heat propagation through the thickness is far better, and defect detection is easier in this method than in one-sided inspection. Therefore, two-sided inspection is a very useful method for defect detection, but not for defect characterization.

6. Conclusions

Theoretical estimation of testing parameters is made for determining optimum conditions for testing 15 mm thick composite laminate. Experiments were performed with optimized parameters in one–sided inspection method. Defects upto a depth of 3.75 mm were detectable in raw IR images by one-sided method. Noise is found to be affecting defect detection. Data processing methods such as phase imaging, normalization and logarithmic fitting methods were found to improve defect detectability. Defects upto a depth of 5.25 mm are detectable in phase image by one-sided inspection. From plot of SNR as a function of defect depth, defect detection limit for15 mm thick laminate has been estimated under optimized testing conditions; maximum defect detection limit is found to be 5.25 mm. Two sided inspection method is found to be useful for detection of deeper defects >5.25 mm (up to 13.5mm).

7. Acknowledgement

Authors gratefully acknowledge Dr Vladimir P Vavilov, Institute of Introscopy, Tomsk Polytechnic, Tomsk Russia for his helpful suggestions and discussions.

8. References

1. Maldague.X and Marinetti.S, “Pulse phase Infrared Thermography” J.Appl. Phys., 79, 2694, 1996
2. Vavilov V.P and Burleigh D.D, *Nondestructive testing handbook*, Vol.3, chapter 3, 54-75, ASNT,2001.
3. Vavilov V.P, *Nondestructive testing monographs and traces*, Vol.7, chapter 5, 131-210,Gordon and Breach science publishers,Great Britain, 1992.
4. Maldague X.P.V., *Theory and practice of Infrared technology for non-destrucive testing*, Johjn Wiley & Sons, New York, USA, 2001.
5. Maldague X.P.V., “Introduction to NDT by Active Infrared Thermography” Materials Evaluation, September, 1060-1073, 2002.
6. Vavilov V.P., “Three dimensional analysis of transient thermal NDT problems by data simulation and processing” Thermosense XXII, SPIE, 4020, 152-162, 2000.
7. Siddiqui A.O, Srinivas K and Lahiri J, “Thermography NDT of thick composites: Part I: Theoretical studies” *Proc. ISNT NDE annual conference , Kolkotta 2005*
8. Srinivas K , Siddiqui A O and Lahiri J, “ Thermography NDT of thick composites:

Part I: Experimental studies" *Proc. ISNT NDE annual conference , Kolkotta 2005*

9. Vavilov V.P., "Accuracy of thermal NDE numerical simulation and reference signal evolutions", *Thermosense XXI* ,SPIE Vol. 3700(1999).
10. Vavilov V.P., X.P.V. Maldague, B. Dufort, J. Robitaille, and J. Picard, "Thermal NDT of Carbon Epoxy composites: detailed analysis and data processing", *NDT&E Intern.*, **26**(2), 85-95, 1993.
11. Shepard S.M., "Advances in Pulsed Thermography", *Thermosense XXIII*, SPIE Vol. 4360, 511-515, 2001.
12. Shepard S.M., Yulin Hou, "Quantitative comparison of Thermographic data sequences", *Materials Evaluation*, 7, 740-745, 2005.